Nanoscale Res Lett (2010) 5:296–301
DOI 10.1007/s11671-009-9479-3

NANO EXPRESS

Biomolecular Nano-Flow-Sensor to Measure Near-Surface Flow

Sang-Wook Lee · Haruyuki Kinoshita · Hiroyuki Noji · Teruo Fujii · Takatoki Yamamoto

Received: 28 August 2009 / Accepted: 28 October 2009 / Published online: 14 November 2009
© to the authors 2009

Abstract We have proposed and experimentally demonstrated that the measurement of the near-surface flow at the interface between a liquid and solid using a 10 nm-sized biomolecular motor of F_1-ATPase as a nano-flow-sensor. For this purpose, we developed a microfluidic test-bed chip to precisely control the liquid flow acting on the F_1-ATPase. In order to visualize the rotation of F_1-ATPase, several hundreds nanometer-sized particle was immobilized at the rotational axis of F_1-ATPase to enhance the rotation to be detected by optical microscopy. The rotational motion of F_1-ATPase, which was immobilized on an inner surface of the test-bed chip, was measured to obtain the correlation between the near-surface flow and the rotation speed of F_1-ATPase. As a result, we obtained the relationship that the rotation speed of F_1-ATPase was linearly decelerated with increasing flow velocity. The mechanism of the correlation between the rotation speed and the near-surface flow remains unclear, however the concept to use biomolecule as a nano-flow-sensor was proofed successfully.

Electronic supplementary material The online version of this article (doi:10.1007/s11671-009-9479-3) contains supplementary material, which is available to authorized users.

S.-W. Lee · H. Kinoshita · T. Fujii
Institute of Industrial Science, University of Tokyo, Fw-601 4-6-1 Komaba Meguro-ku, Tokyo 153-8505, Japan

H. Noji
The Institute of Science and Industrial Research, Osaka University, 8-1 Mihogaoka-Ibaraki, Osaka 567-0047, Japan

T. Yamamoto (✉)
Department of Mechanical and Control Engineering, Tokyo Institute of Technology, Ishikawadai 1-314, Ookayama 2-12-1 Meguro-ku, Tokyo 152-8550, Japan
e-mail: yamamoto@mes.titech.ac.jp

Keywords Microfluidics · Near-surface · F_1-ATPase · Micro-PIV · Flow-sensor

Introduction

Microfluidic systems enable various fluidic operations at micro-scale, which lead enormous possible applications in life science, chemistry, etc. [1–5]. One of the most fundamental but important issue in microfluidic systems is to measure the flow, not only as a function of the system to control precisely the internal flow, but also a scientific interest to probe the interface between liquid and solid near the surface at nanoscale to characterize the near-surface flow experimentally. The importance of near-surface flow is now growing as microfluidic technology progress, because many of the reactions and analyses in microfluidic system use the surface-immobilized functional molecules and catalysts, which are dominated by the transportation of reactants and analytes by diffusion and convection near the surface. And furthermore, such an increased surface-to-volume ratio results in surface-dominated physics; most of the considered domain might be a surface.

Various types of micro flow sensing scheme has been extensively studied for the microfluidic systems; a cantilever distortion caused by hydrodynamic force [6, 7], Coriolis force induced twisting angular motion [8], miniaturized thermal anemometers [9, 10], etc. These embedded types of sensors are mainly intended to measure the bulk flow, however, not to probe the near-surface flow.

On the other hand, not sensor but velocimetry, flow velocity profiles near the surface have been measured experimentally using microscopic particle image velocimetry (micro-PIV) [11, 12], fluorescence correlation spectroscopy coupled micro-PIV [13], and near-field optics

coupled micro-PIV, in which an evanescent wave is used to visualize only the proximity of surface [14]. Although it is expected to be a practical means of measurement now, the resolution perpendicular to the surface is limited to hundreds nanometers because of the difficulty in controlling the evanescent depth, and the difficulty in capturing the particle image if the particles are less than a few hundreds of nanometers caused by its very fast Brownian motion and weak fluorescence.

Herein, we propose a concept that is the use of a biomolecular motor protein of F_1-ATPase as a nano-flow-sensor to measure the flow velocity in the proximity of a solid surface. In fact, F_1-ATPase functions as a rotary molecular motor in a living body; the central γ-subunit rotates anticlockwise against $\alpha_3\beta_3$-subunits by hydrolysis of ATP [15]. Because the size of F_1-ATPase is about 10 nm, much less than the detection limit of an optical microscope, its rotation has been observed by coupling the γ-subunit to a nanometer-sized tag-bead that enhances the rotational motion. Our idea is that, if a flow near a surface exerts a hydrodynamic force on the F_1-ATPase and the tag-bead complex (F_1-bead) that is immobilized on a considered surface, the rotational motion will be affected and correlated with the near-surface flow. Therefore, the near-surface velocity can be evaluated directly if the rotation of F_1-bead is measured. Using a biomolecule as kind a nano-machine might sound impractical idea, because biomolecule is usually unstable, irreproducible, etc. Realizing practical artificial nano-machine (nano-flow-sensor in this case) is a different issue and is technological improvements on the immediate horizon. Using forthcoming F_1-ATPase is only the way to utilize nano-machine for near-surface flow measurements at present, and we believe that the obtained knowledge will be profitable for the future development of such a nano-machine and the related applications in nanotechnology.

This article presents the first demonstration to show the concept of measuring near-surface flow using biomolecular motor of F_1-ATPase as a nano-flow-sensor.

Experimental

The theoretical resolution in surface-normal direction can be down to around 10 nm of the size of F_1-ATPase, whereas the practical resolution could be limited by the size of the tag-bead immobilized on F_1-ATPase. It is therefore important to optimize the size and the shape of the tag-bead to get closer to the theoretical resolution. However, developing the tag-bead is a different technological aspect of this concept. This work is intended to prove the concept to use F_1-ATPase as a nano-flow-sensor. Therefore, we used an easily observable sized commercially available tag-bead to demonstrate in this work; even though the resolution is not high enough to be comparable to the recent near-field optics coupled micro-PIV techniques.

Microfluidic chip

We developed a microfluidic test-bed chip consisting of three sub-chips to precisely control the liquid flow acting on the complex of F_1-ATPase and bead (F_1-bead) immobilized on a surface, as schematically illustrated in Fig. 1. The microfluidic chip design resembles that of our previously developed one, in which the Si-based micropump chip [16], the polydimethylsiloxane (PDMS)-based microchannel chip, and the Ni–NTA coated glass-made immobilization chip are integrated [17]. The cross-section size of the microchannel is 800 μm wide and 60 μm deep, which is connected through the micropump. The observation area of the device is entirely transparent, so that the rotation of F_1-bead is visible by transparent light through the device under an optical microscope. The F_1-ATPase used here was a genetically modified one having 6 His-tags at the bottom of $\alpha_3\beta_3$-subunits (stator of motor), whereas at the top of the γ-subunit (rotor of motor) was biotinylated to have a single biotin molecule. Because His-tag binds particularly to Ni–NTA and biotin binds to avidin, the bottom of F_1-ATPase is immobilized on the surface of the Ni–NTA coated immobilization chip; an avidin-coated bead is immobilized at the top of the γ-subunit, as depicted in Fig. 1b. It is noteworthy that, because the bead is a spheroid having rotation symmetry, it is difficult to detect the rotation if it rotates on its axis with no axial run out. Therefore, we specifically examined only the duplex bead, which is statistically obtained by repeated centrifugal aggregation and dispersion. The duplex bead strongly enhances the rotation for visualization and also enhances the interaction with the fluid motion because of its off-axis rotation, as depicted in Fig. 1b.

Flow Evaluation

In the micro-PIV measurement, fluorescent beads (R500; Duke Scientific Corp.) with an average diameter of 500 nm were used as tracer particles. The bead emits red light (emission maximum: 612 nm) when illuminated by green light (excitation maximum: 542 nm). The focal plane of the micro-PIV was set at the middle height of the microchannel (30 μm distant from the surface) to find the bulk flow velocity. The rotation plane of the F_1-bead is assumed at 200 nm from the surface; theoretically, the F_1 height is about 10 nm, the bead (ϕ350 nm, CM01 N/7024; Bangs Laboratories Inc.) radius is about 175 nm, and the avidin layer on the bead is expected to be a few nanometres thick, which corresponds to approximately 200 nm or less distant

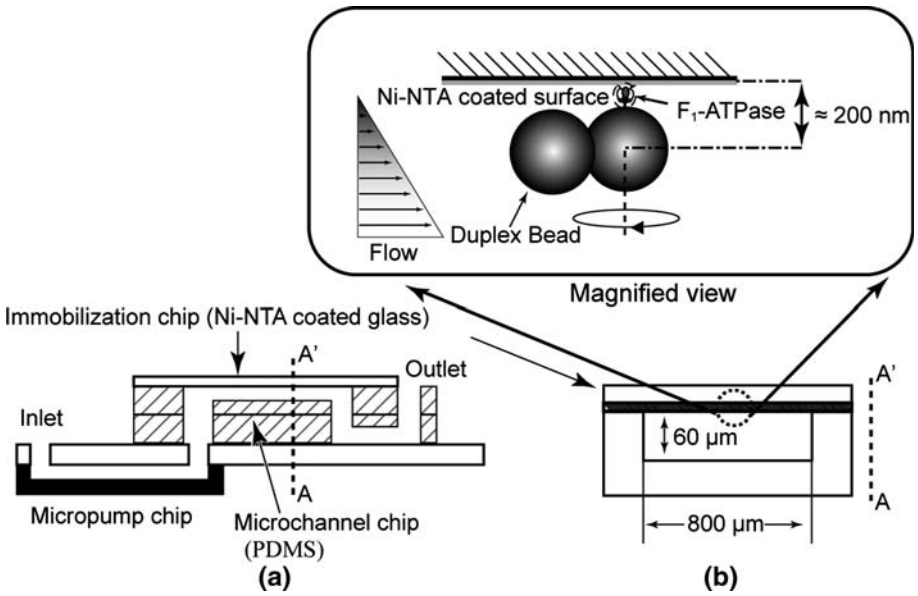

Fig. 1 Design of microfluidic chip. **a** Side view of the microfluidic chip that is assembled three sub-chips, micropump chip, immobilization chip, and microchannel chip into a single functional chip. **b** Cross-section at A–A′ plane of panel **a**, showing the shape and dimension of the microchannel. The F_1-ATPase-bead conjugate is immobilized upside down on the inner surface of the immobilization chip

from the surface. The F_1-bead rotation must be correlated by a flow at near-surface 200 nm apart from the wall. It was, however, impossible to obtain the velocity profile at 200 nm apart from the wall by micro-PIV directly with our experimental apparatus. Therefore, the rotation of F_1-bead was primitively evaluated by comparing the mean flow velocity in the microchannel obtained by the micro-PIV. The near-surface velocity at 200 nm from the wall was also very roughly estimated by extrapolating a parabolic profile of the assumed Poiseuille-like flow ($Re \approx 0.01$) if the boundary is no-slip.

Consequently, the focal plane of the micro-PIV measurement and that of the F_1-bead rotation were 30 μm and 200 nm apart from the bottom wall, respectively. Because the focal depth of the objective lens (UPLSAPO ×100 NA 1.4; Olympus Co.) with the camera (1/2 inch 3CCD ExwaveHAD; Sony Inc.) is less than 1 μm for the F_1-bead observation, it is impossible to visualize the both at the same time. Furthermore, the micro-PIV particles hit and stopped the rotation of F_1-bead when micro-PIV and F_1-rotation are conducted at the same time. Therefore, we conducted micro-PIV and F_1-bead rotation separately but sequentially using the same microchannel.

Sample Preparation and Measurement

The microfluidic chip was mounted on an *x*–*y* translation stage located under an epi-fluorescent microscope (BX-50-FM-RFL; Olympus Corp.). We used cameras of two types for the experiment. One is a high-speed and high-sensitive camera (Phantom v.7.1; Vision Research Inc.) for micro-PIV measurements. The other is an ICCD camera (M4314; Hamamatsu Photonics Inc.) to visualize the F_1-bead rotation.

The rotation assay of the F_1-bead was conducted using the following procedures. A buffer solution [10 mM 4-morpholinepropanesulfonic acid (MOPS)–KOH/50 nm KCl 1% (vol/vol) BSA, pH 7.0] was flowed thoroughly to fill the entire microchannel at the first step. Second, 2 nM biotinylated His-tagged F_1-ATPase in the buffer solution was introduced to the microchannel and was immobilized naturally to Ni–NTA on the surface for a few minutes. Streptavidin-coated duplex bead (ϕ350 nm, CM01 N/7024; Bangs Laboratories Inc.) solution was then flowed continuously to attach itself naturally to the biotinylated part of F_1-ATPase to be F_1-bead complex for 15 min. Finally, 700 μM ATP in the buffer solution was introduced to start rotation. The rotational motion was extracted automatically from the video image using homemade image processing software on a PC.

Results

Figure 2 shows the relationship between the rotation speed of four different randomly chosen F_1-beads and the mean velocity $u_{m,}$ and the estimated near-surface velocity u_F. Apparently, the linear correlations are obtained between the rotation speed of F_1-beads and the flow velocity, even though the intercept of the graphs varies widely across the samples. The rotation was stopped at a mean velocity of more than 1.1 mm/s.

In order to elucidate why and how the F_1-bead rotation is correlated with the near-surface velocity, we made a detailed plot at mean velocity $u_m = 0$, 10.5, 16.0, and 23.8 μm/s, as shown in Fig. 3. The four graphs depict the time course of the rotation of F_1-bead at each mean

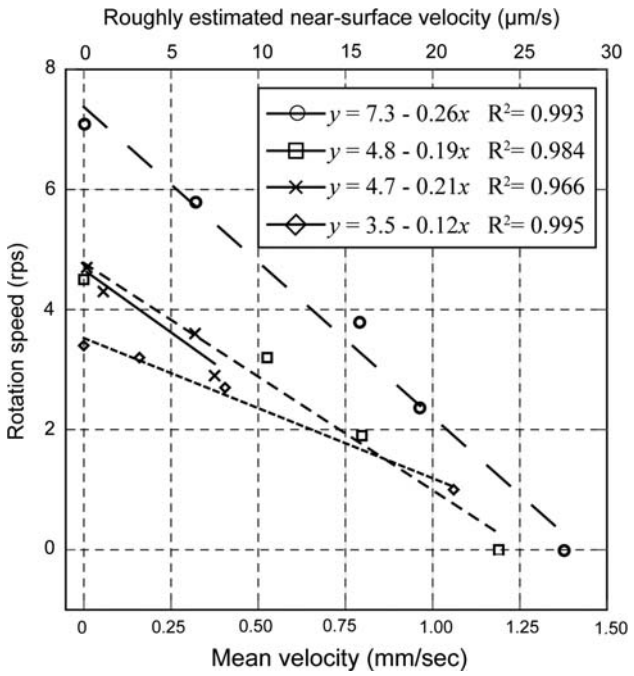

Fig. 2 Relationship between rotation of F_1-bead and near-surface velocity. Four randomly chosen F_1-beads were investigated to obtain the relationship between rotation of F_1-bead and near-surface velocity. The velocity dependence of F_1-bead rotation is widely varied across samples, especially the intercept. However, the tendency of linear correlations is obtained from all of them

velocity. The slopes of the graph represent the rotation speed of F_1-bead, which decreases with increasing the mean velocity. The insets show the centroid plot of the bead position at 33 ms time intervals; the black dots show the presence of bead at each measured moment. The F_1-bead rotates counter-clockwise by the nature of F_1-ATPase, as indicated by the arrow. As shown there, the F_1-bead is almost uniformly rotated if no-flow exists (Fig. 3a), although several regions exist which are slower or faster than the others, which appeared as the dense or the sparse dots if the flow is present, as shown in Fig. 3b, c. I It is qualitatively expected that the rotation in the upper half will be decelerated while the lower half will be accelerated because of the relative configuration between the direction of flow and the rotation. For Fig. 3b at the slower flow condition, the F_1-bead is the most decelerated at around 90° at an angle to the flow streamline, whereas it is the most accelerated at around 270°. For the faster flow, both most decelerated and accelerated regions appear as a bit shifted to (and making an acute angle with) the flow direction.

These results can be modeled if it is considered as the Stokes resistance in the rotation of a sphere about a non-centrally located axis under a uniform flow; the resistant torque T may be very roughly evaluated as $T = -8\pi\eta a^2\omega - 6\pi\eta ar\omega$, where η is the viscosity, a is the bead diameter, r is the rotation radius, and ω is the angular velocity [18]. However, because the flow is presumed to be uniform (from left to right in the figures), the decelerated and accelerated effects must counteract each other, meaning that the presence of flow does not affect the rotation speed with this simple model. We therefore presume that it can result from the following: (1) deformation of the molecular structure of F_1-ATPase by external hydrodynamic force deteriorates the activity of F_1-ATPase itself; (2) non-negligible friction exists between the bead and the surface by an inappreciable inclination of the rotation axis by the applied hydrodynamic force; or (3) both of (1) and (2).

To evaluate those hypotheses, tag-bead size dependence of F_1-bead rotation at without flow (0 μm/s) and with flow (51.1 μm/s as near-surface velocity) was measured by varying the size of the tag-bead from 350 to 800 nm. Because it is difficult to obtain a tag-bead (duplex bead) smaller than 350 nm using commercially available beads with our method, the tag-bead size dependence was evaluated as greater than 350 nm. Results show that the rotation of F_1-beads is linearly proportional to tag-bead size both with flow and without flow as shown Fig. 4. As a result, the rotation of F_1-bead is linearly proportional to the tag-bead size, which will implicitly suggest that Stokes resistance may deform the molecular structure of F_1-ATPase and deteriorates the activity of F_1-ATPase and/or may induce an inappreciable inclination of the rotation axis resulting in increase non-negligible friction exists between the bead and the surface.

Conclusions

This method remains in the primitive experimental stage, so that there many problems should be solved for quantitative measurement and practical use, especially to improve depth resolution and to understand behind mechanism. However, our concept to use a bimolecular motor of F_1-ATPase as a nano-flow-sensor was demonstrated successfully. The measurement limit of the flow sensing is currently less than about 1.1 mm/s as mean velocity (correspond to roughly 22 μm/s at 200 nm apart from the surface). The available velocity range can be expanded to the higher range by optimizing the size and the shape of the tag-bead to control applied hydrodynamic force from the flow. Optimization by decreasing the tag-bead size will also lead to higher depth resolution, which can be as small as the size of F_1-ATPase of 10 nm or bit larger tens nm. For example, a biomolecule of rod-shaped actin filament with the diameter of 10 nm [19], a rod-shaped colloidal gold with the diameter of 39 nm [20], and a single spherical colloidal gold with the diameter of

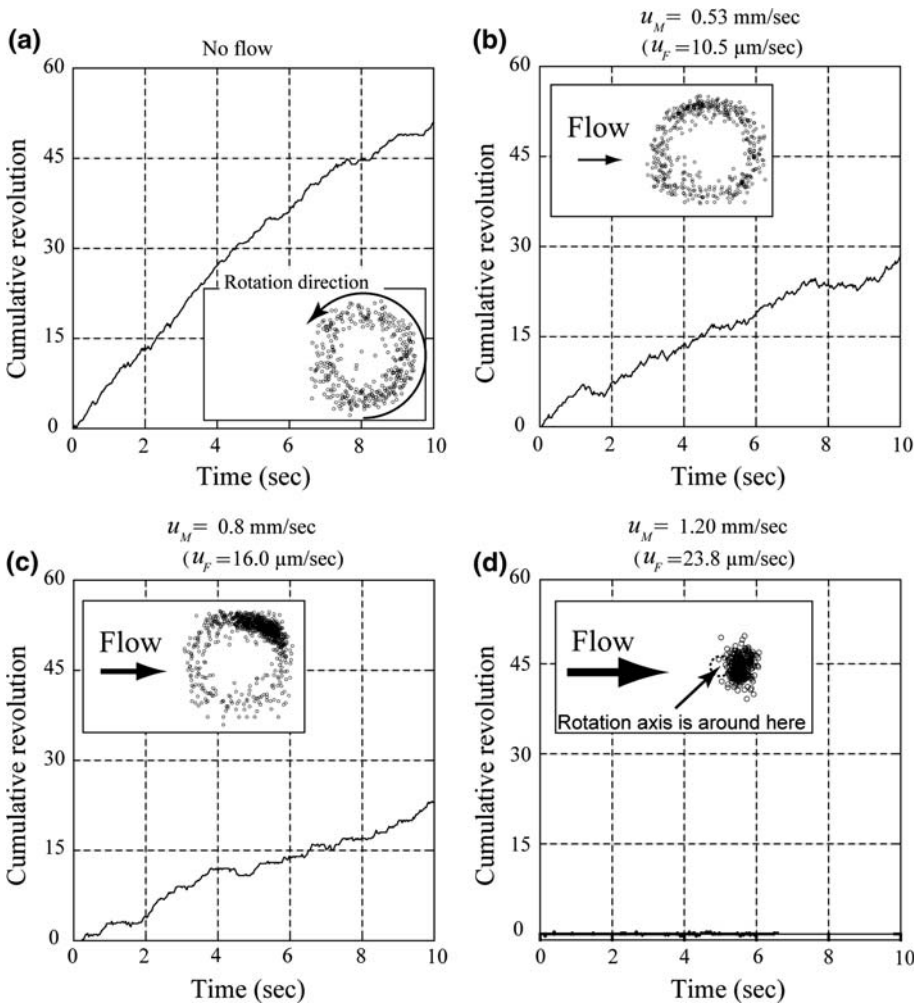

Fig. 3 Time course of the velocity dependency of F_1-bead rotation. F_1-bead rotations are measured at four different near-surface velocities. The *insets* show the centroid plot of the bead position at 33 ms intervals. In the experiment, the rotation is halted at more than 22 μm/s (data not shown)

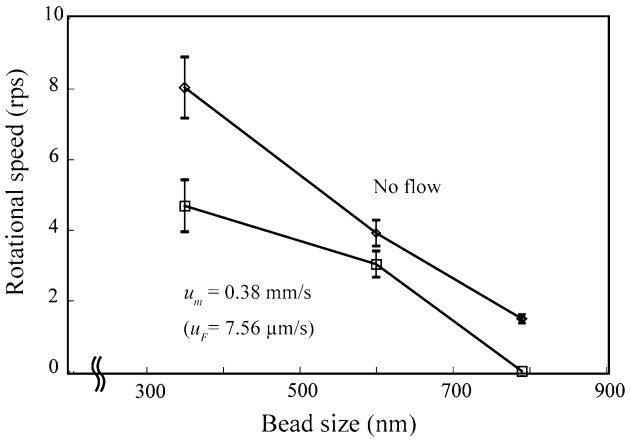

Fig. 4 Tag-bead size dependence of F_1-bead rotation. The size dependence of F_1-bead rotation was measured without flow and with flow (0.38 μm/s) by varying the size of the tag-bead from 350 to 800 nm. In both cases, the rotation of F_1-bead is linearly proportional to the tag-bead size

40 nm or less [21] have already demonstrated to visualize F_1-ATPase rotation under no-flow condition. By using these tag-bead technologies, the depth resolution will be much higher into really tens nanometer region at near-surface. Furthermore, our speculation about the mechanism of the velocity-dependent rotation F_1-bead can be evaluated through such optimization by controlling the interaction not only between the tag-bead and flow, but also between the tag-bead and the surface by immobilizing F_1-bead onto a nano-fabricated relief structures to control their mutual friction.

Using biomolecule as a nano-tool has many problems for practical use at present. It would be solved by merging future nanotechnology to realize artificial nano-machines. Whichever biomimetic or fully artificial design, we believe that the knowledge obtained from biomolecular nano-machine would be helpful to realize such a future nanotechnology.

Acknowledgments This work was supported by the Japan Society for the Promotion of Science, Bio-Oriented Technology Research Advancement Institution, a Grant-in-Aid for Scientific Research (20510114) from the Ministry of Education, Culture, Sports, Science and Technology, and Precursory Research for Embryonic Science and Technology from Japan Science and Technology Agency, Japan.

References

1. B.H. Weigl, R.L. Bardell, C.R. Cabrera, Adv. Drug Deliv. Rev. **55**, 349 (2003)
2. T.M. Squires, S.R. Quake, Rev. Mod. Phys. **77**, 977 (2004)
3. D. Janasek, J. Franzke, A. Manz, Nature **442**, 374 (2006)
4. H. Craighead, Nature **442**, 387 (2006)
5. D.B. Weibel, G.M. Whitesides, Curr. Opin. Chem. Biol. **10**, 1 (2006)
6. R. Kersjes, J. Eichholz, A. Langerbein, Y. Manoli, W. Mokwa, Sens Actuators A **37**, 674 (1993)
7. J. Van der Weil, Ph.D. thesis, Institute of Microtechnology, University of Neuchatel, 1994
8. P. Enoksson, G. Stemme, E. Stemme, J. MEMS **6**, 119 (1997)
9. M. Ashauer, H. Glosch, F. Hedrich, N. Hey, H. Sandmaier, W. Lang, Sens. Actuators A **79**, 7 (1999)
10. S. Wu, Q. Lin, Y. Yuen, Y.C. Tai, Sens. Actuators A **89**, 152 (2001)
11. J.G. Santiago, S.T. Wereley, C.D. Meinhart, D.J. Beebe, R.J. Adrian, Exp. Fluid. **25**, 316 (1998)
12. H. Kinoshita, S. Kaneda, T. Fujii, M. Oshima, Lab Chip **7**, 338 (2007)
13. D. Lumma, A. Best, A. Gansen, F. Feuillebois, J.O. Rädler, O.I. Vinogradova, Phys. Rev. E **67**, 056313 (2003)
14. R. Pit, H. Hervet, L. Léger, Phys. Rev. Lett. **85**, 980 (2000)
15. K. Kinosita, R. Yasuda, H. Noji, K. Adachi, Philos. Trans. R. Soc. B. **355**, 473 (2000)
16. T. Fujii, Y. Sando, K. Higashino, Y. Fujii, Lab Chip **3**, 193 (2003)
17. S.W. Lee, T. Yamamoto, H. Noji, T. Fujii, Enzyme Microb. Technol. **39**, 519 (2006)
18. J. Happel, H. Brenner, *Low Reynolds Number Hydrodynamics* (Kluwer, Boston, 1983)
19. R. Yasuda, H. Noji, K. Kinoshita, M. Yoshida, Cell **93**, 1117 (1999)
20. J. York, D. Spetzler, F. Xiong, W.D. Frasch, Lab Chip **8**, 415 (2008)
21. R. Yasuda, H. Noji, M. Yoshida, K. Kinoshita, H. Itoh, Nature **410**, 898 (2001)